Numerical Analysis of Intensity and Phase Noise of Solitary AlGaAs Semiconductor Lasers Operating in Multimode

Sazzad M.S. Imran, Farjana Ferdous Tonni and Sumona Islam Sumi

Abstract—In this paper, both intensity and phase noise of solitary semiconductor lasers operating in multimode has been analyzed. A self-consistent numerical model is used for simulation of the rate equations for photon numbers, its phase and carrier numbers for typical 780 nm AlGaAs lasers. Self-suppression coefficient and both symmetric and asymmetric cross gain suppression coefficients are considered in the analysis. We have also considered Langevin noise sources for the photon number, its phase and carrier numbers which induce instantaneous fluctuation in photon and carrier numbers. We have described the noise effect through numerical simulation of the relative intensity noise (RIN) and frequency or phase noise (FN). The photon number and carrier number variations with injection current have been obtained. Laser linewidth has been calculated for different injection current values. The frequency spectrum of the intensity noise is calculated with the help of fast Fourier transform (FFT). The transient behavior as well as the steady-state response of semiconductor lasers to varying current input is also analyzed because the transient response is significant in determining the noise characteristics of the laser output. Results show that both intensity and phase noise decreases with the increase of the injection current density. Linewidths have been decreasing substantially with increasing injection current as well.

Index Terms— Rate equations, transient response, relative intensity noise, phase noise, linewidth, semiconductor laser, Langevin noise sources, self-suppression coefficient, gain suppression.

1 Introduction

SEMICONDUCTOR lasers are among the most important optoelectronics devices which are the most common type of laser produced. They provide cheap and compact size lasers that have a wide range of applications in fiber optic communications, barcode readers, laser pointers, CD/DVD/Blu-ray reading and recording, laser printing, scanning and increasingly directional light sources. They consist of complex multi-layer structures requiring nanometer scale accuracy and an elaborate design. The performance of a semiconductor laser is adversely affected by the presence of noise [1]. Under certain operating situations, however, semiconductor lasers often show undesired performance characteristics such as instability of lasing modes and generation of extra noise. Their theoretical description is important not only from a fundamental point of view, but also in order to generate new and improved designs. The description can be done at various levels of accuracy and effort, resulting in different levels of understanding. The noise present in the output of laser diodes limit their reliability when applied as light sources in optical communication systems, optical discs, etc. Thus analysis of the noise becomes crucial in improving the efficiency of semiconductor lasers.

There are some theoretical models exist that describe the random amplitude and phase fluctuations in the light generated by semiconductor lasers, including their correlation, well. [1], [2], [3], [4], [5], [6], [7], [8], [9], [10] These models, based on the description of noise through power spectral densities, are extremely useful in modeling the effect that linear processes have on semiconductor laser light. However, the effect of devices or processes that are either nonlinear (e.g. high power transmission on certain types of silica fiber) or not time-invariant (e.g. amplitude and/or frequency modulation) may not always be described in the frequency domain. Our first milestone is the calculations of D. Marcuse, who reported a model of intensity fluctuations in which the Langevin noise sources on the photon and carrier numbers are generated with defined auto- and cross-correlations [2]. In his paper [3], D. Lasaosa *et al.* presented an algorithm designed to produce improved simulations of amplitude and phase fluctuations present in the light output of semiconductor lasers. The algorithm, known as improved time resolved simulation, is based on the physical principle of operation of semiconductor lasers, and takes fully into account the correlation between amplitude and phase fluctuations, as well as mode-partition noise at the laser output. Results obtained, using this algorithm, are then shown to agree with noise descriptions based on the power spectral density. The simulation results agree very well with theoretical predictions since the algorithm mimics the physical processes inherent to laser operation.

Intensity and phase noise on the output of laser diodes limit their reliability when applied as light sources in optical communication systems, optical discs, optical measuring, etc. The quantum noise corresponds to intrinsic fluctuations in the photon number, carrier number and phase that are generated during the quantum interaction processes of the lasing field with the injected charge carriers. Excess noise is

- *Sazzad M.S. Imran is currently an Associate Professor in the Department of Electrical and Electronic Engineering at the University of Dhaka, Bangladesh. E-mail: sazzadmsi@du.ac.bd*
- *Farjana Ferdous Tonni and Sumona Islam Sumi are currently pursuing masters degree program in the Dept. of Electrical and Electronic Engineering at the University of Dhaka, Bangladesh. E-mail: tonni90@yahoo.com and sumonasumi99@yahoo.com*

generated when other effects, such as the re-injection of light by optical feedback, amplify the intrinsic fluctuations. Analysis of the laser noise is necessary for further improvement of the device performance. In the paper [4], M. Ahmed *et al.* reported a self-contained numerical model to analyze the intensity and phase noise and broadening of the line shape. Authors demonstrated a systematic technique to generate the Langevin noise sources on the photon number, carrier number and phase while keeping their auto- and cross-correlations satisfied. The technique could be understood as a generalization of the method by Marcuse [2]. The time variations of fluctuating photon number, carrier number and phase are analyzed and their statistics as well. Frequency spectra of both intensity and phase noise are calculated with the help of the fast Fourier transform (FFT). The noise results are compared with those predicted by the small-signal analysis [5], [6], [7], [8], [9], [10], [11], [12], [13], [14]. Authors suggested that their proposed model can be applied to analyze complicated phenomena under optical feedback with suitable extensions of the model.

In this paper, a self-consistent numerical model is to be applied to analyze the intensity and phase noise of 780 nm AlGaAs lasers. The rate equation model for photon numbers, carrier numbers and optical phase for semiconductor laser operating in multimode are determined considering nonlinear gain coefficients. The parameters of the rate equations for typical AlGaAs are used for numerical simulation to demonstrate the noise characteristics. The noise effect is described through relative intensity noise (RIN) and frequency or phase noise (FN). The variation of linewidth for different injection current is explained. Time varying profiles for the photon number, carrier number and phase fluctuation or frequency variation are demonstrated. The average photon number and average carrier number variations with injection current are also shown.

The following section lays down the theoretical model of our analysis. This part forms the basis of the work to be done in this paper. It talks about the rate equations for photon number and carrier number and also about the introduction of noise sources. After the development of the algorithm for numerical simulation in Matlab using Runge-Kutta method of the fourth order, we discuss the various results of the simulation for the laser rate equations and analyze them in the third section. Finally, the paper ends up with some concluding remarks on the results.

2 Theoretical Model of Analysis

2.1 Laser Rate Equations for Photon Number, Its Phase and Carrier Number

The present noise analysis of the solitary semiconductor lasers is based on the following multimode rate equation model of the injected carrier number $N(t)$ and modal photon number $S_p(t)$ and photon phase $\theta_p(t)$ with p= 0, ±1, ±2,…, ±6.

For photon numbers:

$$\frac{dS_p}{dt} = \left(G_p - G_{tho}\right)S_p + \frac{\xi aN/V}{\left[2\left(\lambda_p - \lambda_0\right)/\delta\lambda\right]^2 + 1} + F_{Sp}(t) \tag{2.1}$$

For photon phase:

$$\frac{d\theta_p(t)}{dt} = \frac{1}{2}\left[\frac{\alpha a\xi}{V}\left(N - \overline{N}\right)\right] + F_{\theta p}(t) \tag{2.2}$$

For injected carrier (electron) numbers:

$$\frac{dN}{dt} = -\sum_p A_p S_p - \frac{N}{\tau_s} + \frac{I}{e} + F_N(t) \tag{2.3}$$

where G_{tho} is the threshold gain of solitary laser given by,

$$G_{tho} = \frac{c}{n_r}\left[k + \frac{1}{2L}\ln\frac{1}{R_f R_b}\right] \tag{2.4}$$

and G_p is the gain of mode p whose wavelength is λ_p. G_p is defined such that the suppression by mode p itself and both the symmetric gain suppression (SGS) and asymmetric gain suppression (AGS) by other modes $q \neq p$ are taken into account. [4], [15]

$$G_p = A_p - B_p S_p - \sum_{p\neq q}\left(D_{p(q)} + H_{p(q)}\right)S_q \tag{2.5}$$

Here A_p is the linear gain, B_p is the coefficient of self-suppression, and $D_{p(q)}$ and $H_{p(q)}$ are coefficients of SGS and AGS, respectively. These coefficients are given by,

$$A_p = \frac{a\xi}{V}\left[N - N_g - bV\left(\lambda_p - \lambda_0\right)^2\right] \tag{2.6}$$

$$B_p = \frac{9}{4}\frac{\hbar\omega_p}{\varepsilon_0 n_r^2}\left(\frac{\xi\tau_{in}}{\hbar V}\right)^2 aR_{cv}^2\left(N - N_s\right) \tag{2.7}$$

$$D_{p(q)} = \frac{4}{3}\frac{B_p}{\left(2\pi c\tau_{in}/\lambda_p^2\right)^2\left(\lambda_p - \lambda_q\right)^2 + 1} \tag{2.8}$$

$$H_{p(q)} = \frac{3\lambda_p^2}{8\pi c}\left(\frac{a\xi}{V}\right)^2\frac{\alpha\left(N - N_g\right)}{\lambda_q - \lambda_p} \tag{2.9}$$

Other parameters are:

a = differential gain coefficient,
ξ = field confinement factor,
V = volume of the active region,
L = length of the active region,
α = linewidth enhancement factor,
$\overline{N}$ = time average value of $N(t)$,
τ_s = average electron lifetime,
I = injection current,
e = electron charge,
k = internal loss of the laser cavity,
N_g = electron number at transparency,
$\hbar$ = reduced Planck constant,
$\omega_p = 2\pi c/\lambda_p$ *is* the angular frequency of mode p,
τ_{in} = electron intraband relaxation time,
R_{cv} = dipole moment and
N_S = electron number characterizing self-suppression coefficient.

The functions $F_S(t)$, $F_\theta(t)$ and $F_N(t)$ are Langevin noise sources for photon numbers, its phase and carrier numbers, respectively. They are added to the rate equations to account for intrinsic fluctuations of the laser associated with quantum transitions of electrons between the valence and conduction bands [16].

These noise sources are given by,

$$F_{Sp}(t) = \sqrt{\frac{V_{SpSp}}{\Delta t}}.g_s \tag{2.10}$$

$$F_{\theta p}(t) = \sqrt{\frac{V_{SpSp}}{\Delta t}}.\frac{1}{2(S_p+1)}.g_\theta \tag{2.11}$$

$$F_N(t) = \sqrt{\frac{V_{NN}(t)+\sum_p K_p V_{SpN}(t)}{\Delta t}}.g_N - \sum_p K_p F_{Sp}(t) \tag{2.12}$$

The variances are defined as,

$$V_{SpSp} = \left\{\frac{\xi a}{V}(N+N_g)+G_{th}\right\}S_p + \frac{\xi a N}{V} \tag{2.13}$$

$$V_{SpN} = -\frac{\xi a}{V}\{(N+N_g)S_p + N\} \tag{2.14}$$

$$V_{NN} = \frac{\xi a}{V}(N+N_g)\sum_p S_p + \frac{N}{\tau_s} + \frac{I}{e} \tag{2.15}$$

$$K_p = -\frac{V_{SpN}}{V_{SpSp}} \tag{2.16}$$

g_s, g_θ and g_N are random number generations in ranges of, $-1 \le g_s \le 1$, $-1 \le g_\theta \le 1$ and $-1 \le g_N \le 1$

Δt is the time-step of the calculation.

The central mode p=0 with wavelength λ_0 is assumed to lie at the peak of the gain spectrum, and the wavelength of the other modes is defined as,

$$\lambda_p = \lambda_0 + p\Delta\lambda = \lambda_0 + p\frac{\lambda_0^2}{2n_r L} \qquad p = 0,\pm1,\pm2,... \tag{2.17}$$

2.2 Noise and Spectral Linewidth

The frequency content of the mode fluctuations is measured in terms of RIN, which is calculated from the fluctuations $\delta S(t) = S(t_i) - \bar{S}$ in the total photon number.

where $S(t_i) = \sum_p S_p(t_i)$ with $\bar{S} = \frac{\sum S(t)}{\sum t}$.

The noise is calculated from the Fourier frequency components [17]. The RIN and FN spectrum can be originally defined as the Fourier transform of the autocorrelation function written as,

$$RIN = \frac{1}{\bar{S}^2}\frac{\Delta t^2}{T}\left|FFT[\delta S(t_i)]\right|^2 \tag{2.18}$$

$$FN_p = \frac{\Delta t^2}{T}\left|FFT[\Delta\nu_p(t_i)]\right|^2 \tag{2.19}$$

where variation of the optical phase is given as,

$$\Delta\nu_p(t_i) = \frac{1}{2\pi}\frac{d\theta_p}{dt} = \frac{1}{2\pi}\frac{\Delta\theta_p(t_i)}{\Delta t} \tag{2.20}$$

and $$\Delta\theta_p(t_i) = \theta_p(t_i) - \theta_p(t_{i-1}) \tag{2.21}$$

Laser linewidth is the full-width at half-maximum (FWHM) spectrum of the laser operating in single-mode. It is determined from the low frequency component of the frequency or phase noise as,

$$\Delta F = 4\pi FN\big|_{\omega=0} = \frac{eG_{th}^2(1+\alpha^2)}{2\pi\left(I - \frac{I_g}{I_{th}}\right)(I - I_{th})} \tag{2.22}$$

where $I_g = \frac{eVN_g}{\tau_s}$ = current at transparency.

3 Numerical Simulation and Discussion

The aim of the authors is to obtain the photon number $S_p(t)$, phase number $\theta_p(t)$ and carrier number $N(t)$ and corresponding noise terms through numerical simulation. The fourth order Runge-Kutta [2], [3], [4], [5] algorithm has been used to solve the rate equations to obtain the results. For the numerical integrations, a short time interval of Δt=5 ps has been used. Such a small value of Δt produces noise sources that can approximately describe a white noise spectrum up to a frequency of 200GHz. This is so taken such that the behavior of the laser both before and after relaxation frequency can be studied.

Values of the simulation parameters for 780 nm AlGaAs semiconductor laser are- a = 2.75x10^{-12} m^{3}s^{-1}, b = 3x10^{19} m^{3}A^{-2} , $|R_{cv}|^2$ = 2.8x10^{-57} C^{2}m^2 , $\delta\lambda$ = 23 nm, α = 2.6, ξ = 0.2, τ_{in} = 0.1 ps, τ_s = 2.79 ns, N_s = 1.7x10^8, N_g = 2.1x10^8, V = 100 μm^3, d = 0.11 μm, L = 300 μm, n_r = 3.6, k = 10/cm, R_f = 0.2, R_b = 0.7.

3.1 Fluctuations of Photon and Carrier Numbers

The average number of photons for various modes, calculated at an injection current of 1.7 times the threshold value, is plotted in Fig. 3.1. From the figure it can be seen that the average photon number is maximum for mode number m = +1. This indicates that mode no. m = +1, with wavelength λ_{+1} = 780.3 nm, is the dominant mode. Dominant mode shifts from λ_0 to λ_{+1} due to nonlinear gain suppression.

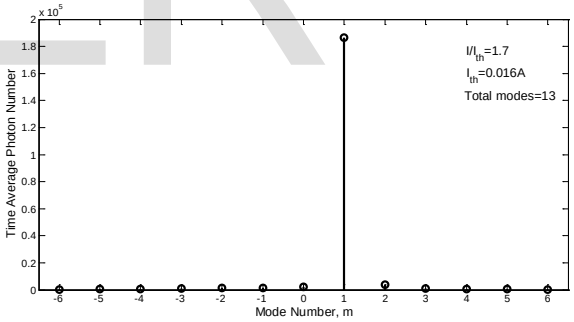

Fig. 3.1: Average number of photons for various modes for injection current $I = 1.7I_{th}$.

Through the numerical simulation, it was possible to obtain and plot the time varying profiles of the photon number $S_p(t)$ for various modes, total photon number $S(t)$ and the carrier number $N(t)$. Figs. 3.2, 3.3 and 3.4 show these profiles for an injection current I equal to 1.7 times the threshold value I_{th}. Figs. 3.2(a) and 3.3(a) show the profile before termination of transients for photon number variations and fig. 3.4(a) shows carrier number variations. Figs. 3.2(b) and 3.3(b) show the profile for steady state response after termination of the transients for photon number fluctuations and fig. 3.4(b) shows carrier number fluctuations. It is important to analyze total photon number variation, because combined photon number gives us the laser output power and practically we cannot separate different modes at the laser output.

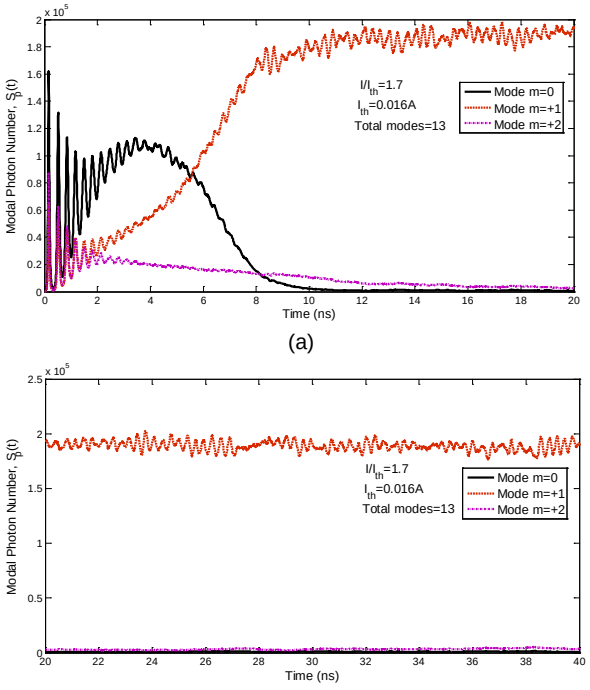

Fig. 3.2: Time varying profile of photon number. (a) During transient for different modes. (b) After termination of transient for different modes.

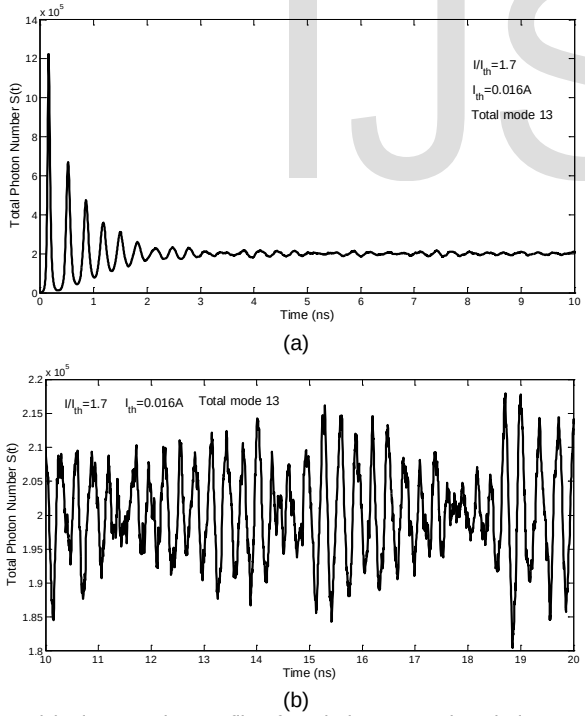

Fig. 3.3: (a) Time varying profile of total photon number during transient. (b) Time varying profile of total photon number after termination of transient.

From Figs. 3.2(a) and (b), it can be seen that initially the fluctuation in photon number has a transient response and we don't get any dominant mode; but after the termination of transients, all the modes fluctuate close to their average values. These fluctuations do not die away, but continue with time even after the transient response has ended. It can also be seen that the profile for steady state response gives us a dominant mode m = +1 and the photon number is maximum for this mode no. +1. The other modes are well suppressed by self and mutual gain suppression mechanisms.

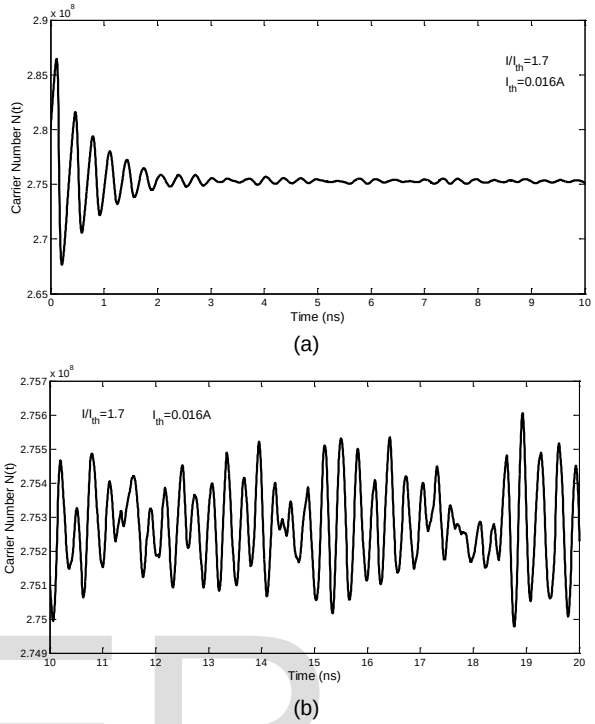

Fig. 3.4: (a) Time varying profile of carrier number during transient. (b) Time varying profile of carrier number after termination of transient.

The same phenomena can be observed for the time varying profiles of the total photon number and carrier (electron) number. Initially, time varying photon number and carrier number show transient response and after few ns transients die away and both total photon number and the carrier number fluctuate around their average values.

To enable comparison and to observe the effect of change in injection current on the time varying profile of photon numbers and electron numbers, Figs. 3.5(a), (b) (c) and (d) were plotted for three different injection currents, $I = 1.3I_{th}$, $I = 1.5I_{th}$ and $I = 1.7I_{th}$. The behavior of these physical quantities before and after the transient response is shown separately.
Figs. 3.5(c) and (d) show that although the average carrier number remains same there is a decrease in the magnitude of the fluctuation with increasing injection current I. This decrease also reflects in the fluctuation of the total photon number [as shown in fig. 3.5(b)], that is, intensity noise decreases with increasing current injection. Fig. 3.5(a) shows that the average photon number increases with increasing injection current; repetition of the photon number fluctuation becomes faster as well, which indicates a shift of the relaxation oscillation frequency towards the higher frequency.

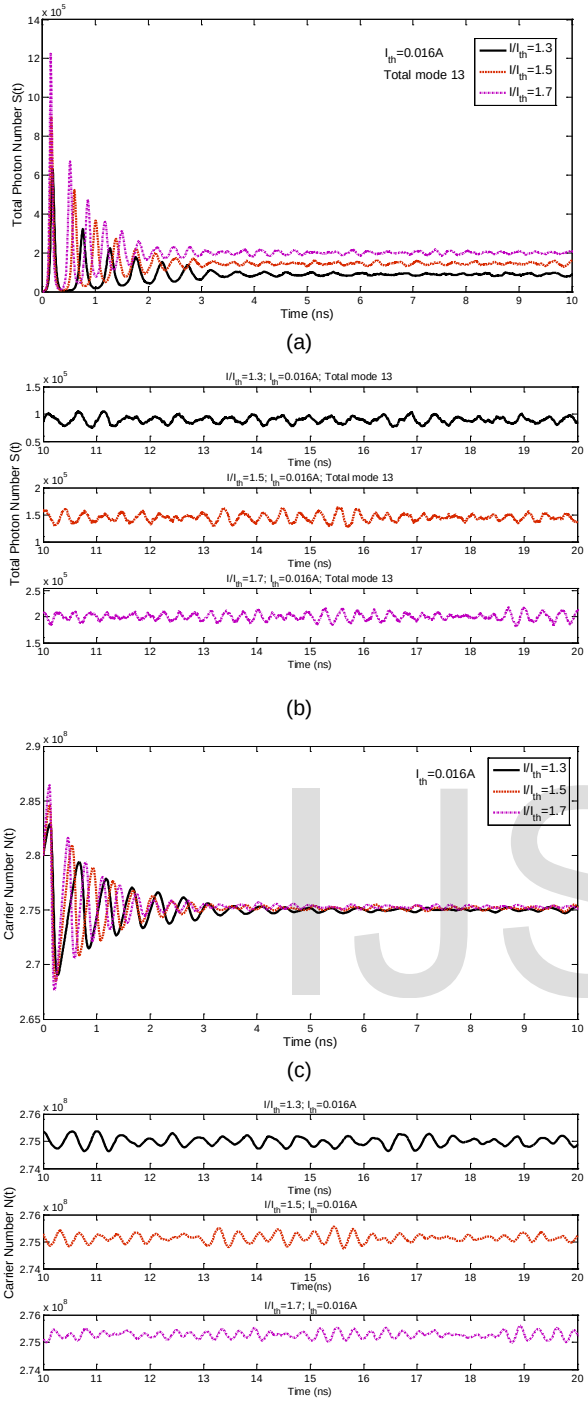

Fig. 3.5: Time varying profiles of total photon and carrier numbers during and after transient response for $I = 1.3I_{th}$, $I = 1.5I_{th}$, $I = 1.7I_{th}$. (a) Transient response of the photon number. (b) Steady-state response of the photon number. (c) Transient response of carrier number. (d) Steady-state response of the carrier number.

3.2 Average Photon and Average Carrier Numbers

It is possible to get time average photon number and carrier number for different injection current I/I_{th} = 0.9, 1.0, 1.1, … through numerical simulation as shown in Figs. 3.6(a) and (b).

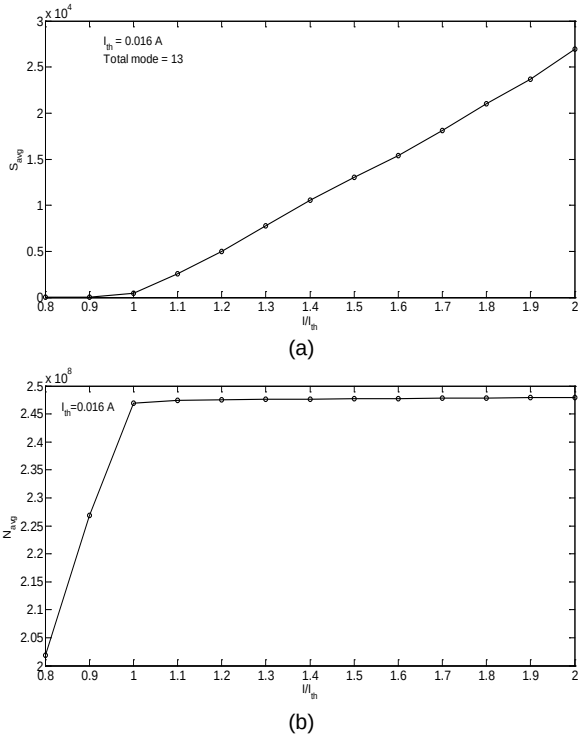

Fig. 3.6: (a) Profile of the average photon number for different values of injection currents. (b) Profile of the average carrier number for different values of injection current.

From Fig. 3.6(a), it can be stated that before the threshold value of injection current $I < I_{th}$, only few photons were generated due to spontaneous emission only and the average photon number was near to 0. But after crossing the threshold value of the injection current $I > I_{th}$, stimulated emission starts and the number of photons generated linearly depends on the carrier injection. Thus the average photon number increases in a linear manner with the injection current I.

From Fig. 3.6(b), it can be seen that before reaching the threshold value, the average carrier number increases very rapidly in a linear manner. After crossing the threshold, stimulated emission starts and as we increase carrier injection more and more carriers recombine to generate photons. Thus average carrier number maintains a constant value.

3.2 Fluctuations of Optical Phase

To enable comparison and to observe the effect of change in injection current on the time varying profile of frequency fluctuations, Figs. 3.7(a) and (b) are plotted for three different injection currents $I = 1.3I_{th}$, $I = 1.5I_{th}$ and $I = 1.7I_{th}$ for the dominant mode m = +1. The behavior of this physical quantity before and after the transient response is shown separately. From the figures, it is seen that fluctuations of the oscillating phase are suppressed and become regular with increasing injection current I. Suppression of phase fluctuations occurs because when the current is far from threshold, the contribution of the random spontaneous transitions to the emitted light can be neglected when compared to the stimulated transitions and hence, the emitted light becomes more coherent.

We consider only dominant mode to calculate the fluctuation of the optical phase of the laser output. Other modes show qualitatively same fluctuation characteristics. This is because for multimode lasers we have to consider phase noise for different modes separately for the optical phase may not even be defined for a laser oscillating on multiple resonator modes. [18]

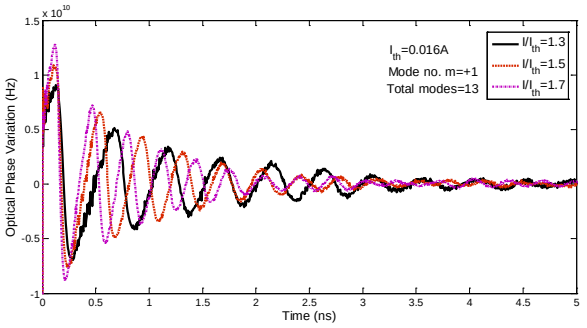

(a)

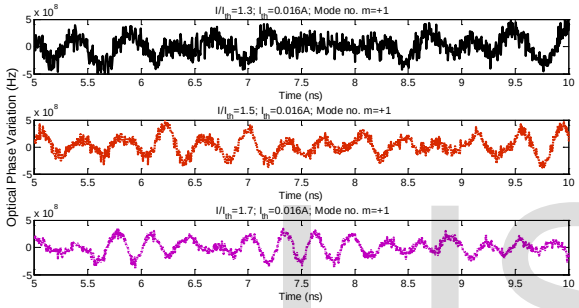

(b)

Fig. 3.7: Time varying profile of optical phase fluctuations for different values of injection currents. (a) During transient state. (b) After transient state.

3.3 Relative Intensity Noise (RIN) & Phase Noise (FN)

In the output of all types of lasers, noise fluctuations are present that are greater than the natural quantum noise of the photon stream. This is because the quantum fluctuations in the electron and photon population are amplified in the optical resonator. This in turn may be attributed to the discrete and random nature of the emission and recombination processes. The effect of fluctuations in the photon and carrier populations on the output of the laser is similar to that in which would be produced by deliberate modulation of the two populations. Complementary processes of photon emission or absorption and electron recombination or generation are correlated in time. All these complementary processes are taken into consideration in our laser rate equations while analyzing the overall effect. The response of the laser to the fluctuation depends on the pumping current. There is a resonant interaction that magnifies the noise over a certain band of frequencies around the relaxation frequency.

Figs. 3.8(a) and (b) show the spectrum of quantum RIN and FN (for the dominant mode m = +1) for injection current $I = 1.7I_{th}$. From the figures we see that both RIN and FN show a pronounced peak around their relaxation oscillation frequency. Spectrum of the RIN and FN are quite flatter at low frequency regime. That shows that the noise characteristics of the laser are affected by the natural resonance of electron and photon populations. Other suppressed modes show qualitatively same FN profile though the noise levels are relatively higher due to more fluctuation of the optical phases.

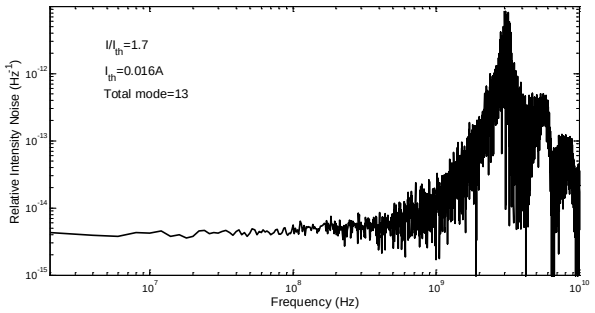

(a)

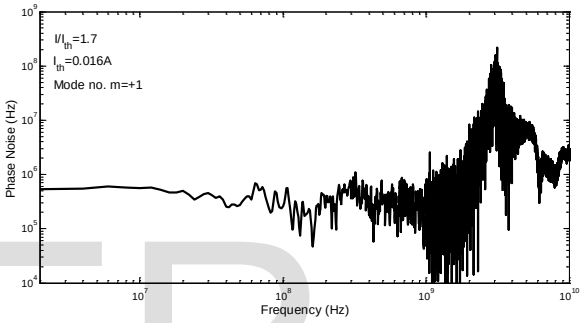

(b)

Fig. 3.8: (a) Frequency spectrum of quantum RIN for $I = 1.7I_{th}$. (b) Frequency spectrum of phase noise (FN) for $I = 1.7I_{th}$.

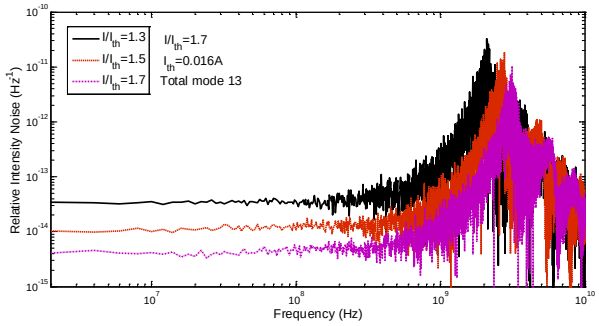

(a)

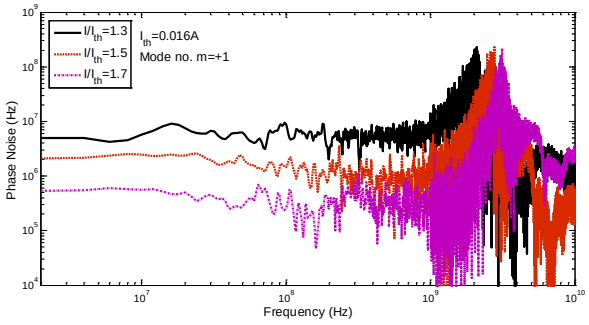

(b)

Fig. 3.9: (a) RIN spectrum for different values of injection current. (b) FN spectrum for different values of injection current.

For a comparative study of the effect of injection current on the RIN and FN spectrum, Figs. 3.9(a) and (b) are obtained for three different values of injection current, for $I = 1.7I_{th}$, $I = 1.5I_{th}$ and $I = 1.3I_{th}$. From the figures it is seen that the increase of the repetition of the photon and carrier fluctuations with increasing injection current I corresponds to a shift of the relaxation oscillation frequency of the RIN and FN spectrum toward the higher frequency side. On the other hand, the suppression of the photon and carrier fluctuations with increasing I leads to a corresponding decrease in the level of the RIN spectrum.

3.3 Laser Linewidth

Laser linewidth can be calculated from the equation (2.22) using FN at very low frequencies due to flatness of FN at lower frequencies. Using phase noise at frequency 200 kHz, laser linewidths for the mode number m = +1 at various injection current were calculated and the profile of linewidth variations with different injection currents was shown in the fig. 3.10.

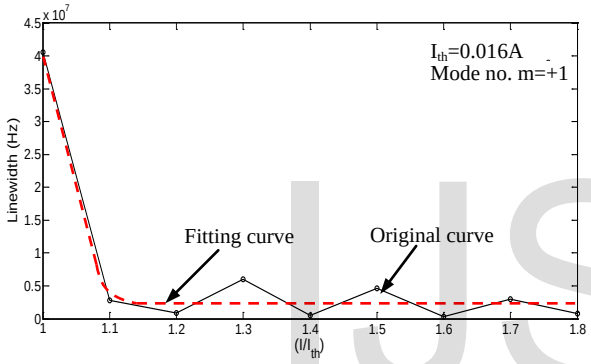

Fig. 3.10: Profile of linewidth variations with different injection currents for mode no m = +1.

Other modes show qualitatively same linewidth variations. The figure proves the rapid narrowing of linewidth Δf with increasing current I near threshold. After stimulated emission or lasing starts, the lasers maintain almost a constant linewidth with increasing current injection. This decrease of the linewidth corresponds to the decrease of the phase fluctuation or frequency noise as evident in Fig. 3.9(b).

4 Conclusion

The obtained results can be summarized as follows.

1) With increasing injection current, there is a shift of the relaxation oscillation frequency towards the higher frequency.

2) It is found that before the threshold value of injection current, only few photons were generated due to spontaneous emission only and the average photon number was near to 0. But after crossing the threshold value of the injection current, stimulated emission starts and the number of photons generated linearly depends on the carrier injection.

3) It is seen that before reaching the threshold value, the average carrier number increases very rapidly in linear manner. After crossing the threshold, average carrier number maintains a constant value.

4) It has been observed that both RIN and FN show a pronounced peak around their relaxation oscillation frequency. Spectrum of the RIN and FN are quite flatter at low frequency regime. The noise characteristics of the laser are affected by the natural resonance of electron and photon populations.

5) With increasing the injection current near threshold, rapid narrowing of laser linewidth is observed. After stimulated emission or lasing starts, the lasers maintain almost a constant linewidth with increasing current injection.

References

[1] Minoru Yamada, "Theory of Semiconductor Lasers From Basis of Quantum Electronics to Analyses of the Mode Competition Phenomena and Noise", Springer Series in Optical Sciences, vol. 185, 2015.

[2] D. Marcuse, "Computer simulation of laser photon fluctuations: theory of single-cavity laser", IEEE J. Quantum Electron., vol. QE-20, no. 10, pp. 1139- 1148, 1984.

[3] D. Lasaosa, M. Vega-Leal and C. Fananas, "Improved time-resolved simulation of amplitude and phase fluctuations in semiconductor laser light", Journal of Opt. Quant. Electron., vol. 40, pp. 367-372, 2008.

[4] M. Ahmed, M. Yamada and M. Saito, "Numerical modeling of intensity and phase noise in semiconductor lasers", IEEE J. Quantum Electron., vol. 37, no. 12, pp. 1600-1610, 2001.

[5] D. E. McCumber, "Intensity fluctuations in the output of CW laser oscillators," Phys. Rev., vol. 141, pp. 306–322, 1966.

[6] H. Haug, "Quantum-mechanical rate equations for semiconductor lasers," Phys. Rev., vol. 184, pp. 338–348, 1969.

[7] T. Paoli, "Near-threshold behavior of the intrinsic resonant frequency in a semiconductor laser," IEEE J. Quantum Electron., vol. QE-15, pp. 807–812, 1979.

[8] G. Arnold and K. Petermann, "Intrinsic noise of semiconductor lasers in optical communication systems," Opt. Quantum Electron., vol. 12, pp.207–219, 1980.

[9] C. H. Henry, "Theory of the phase noise and power spectrum of a single mode injection laser," IEEE J. Quantum Electron., vol. QE-19, pp. 1391–1397, 1985.

[10] C. H. Henry, "Phase noise in injection lasers," IEEE J. Lightwave Technol., vol. LT-4, pp. 298–311, 1986.

[11] M. Yamada, "Theory of mode competition noise in semiconductor injectionlasers," IEEE J. Quantum Electron., vol. QE-22, pp. 1052–1059, 1986.

[12] M. Yamada, "Theoretical analysis of line-broadening due to mode-competitionand optical feedback in semiconductor injection lasers," Trans. IEICE, vol. E71, pp. 152–160, 1988.

[13] G. P. Agrawal and G. R. Gray, "Intensity and phase noise in microcavitysurface-emitting semiconductor lasers," Appl. Phys. Lett., vol. 59, pp. 399–402, 1991.

[14] M. Yamada, "Variation of intensity noise and frequency noise with the spontaneous emission factor in semiconductor lasers," IEEE J. Quantum Electron., vol. 30, pp. 1511–1519, 1994.

[15] M. Ahmed, "Numerical characterization of intensity and frequency fluctuations associated with mode hopping and single-mode jittering in semiconductor lasers", Physics D, vol. 176, pp. 212, 2003.

[16] Paul L. Evries and Javier E. Hasbun, "A first course in computational physics", Second Edition, Jones and Bartlett Publishers, 2011.

[17] C. Serrat and C. Masoller, "Modeling spatial effects in multi-longitudinal-mode semiconductor lasers", Physical Review A, vol. 73, pp. 043812 (1-6), 2006.

[18] R. Paschotta, H.R. Telle and U. Keller, "Noise of Solid State Lasers", Solid-State Lasers and Applications, CRC Press, Boca Raton FL, Chapter 12, pp. 473–510, 2007.